Inorg. Chem. **2002**, *41*, 2927–2935

Solvation Largely Accounts for the Effect of *N*-Alkylation on the Properties of Nickel(II/I) and Chromium(III/II) Cyclam Complexes

Timothy Clark,*,† Matthias Hennemann,† Rudi van Eldik,*,‡ and Dan Meyerstein*,§,||

Computer-Chemie-Centrum der Universität Erlangen-Nürnberg, Nägelsbachstrasse 25, 91052 Erlangen, Germany, Institut für Anorganische Chemie der Universität Erlangen-Nürnberg, Egerlandstrasse 1, 90158 Erlangen, Germany, The College of Judea and Samaria, Ariel, Israel, and Department of Chemistry, Ben-Gurion University of the Negev, Beer-Sheva, Israel

Received December 27, 2001

The source of the effect of *N*-alkylation on the redox properties of Ni(II/I) and Cr(III/II) cyclam complexes has been investigated using DFT calculations. The structures of the anhydrous and hydrated complexes were optimized in the gas phase, and single point calculations were performed in a polarized continuum. The main results are the following: the decrease in outer sphere solvation upon *N*-alkylation is the major source of the relative stabilization of the lower oxidation state complexes by the tertiary amine ligands; tertiary amine nitrogen donors are stronger σ-donors than the secondary amines, as predicted from the inductive effect of alkyls; steric strain elongates the metal–nitrogen bonds in the tertiary complexes and decreases the ligand strain energies; and the site of water binding to the complexes differs because of their different electronic structures (i.e., in the Ni complexes, the water molecules bind to the M–N–H sites, whereas in the Cr complexes they bind to the central metal cation). Outer sphere hydrogen bonding of water to the ligands in the coordination sphere lowers the ionization potentials by charge delocalization.

Introduction

A comparison of the properties of transition metal complexes with tertiary amine ligands with those of the corresponding secondary and primary amines reveals several remarkable effects of *N*-alkylation of the ligands. First, tertiary amine ligands stabilize low valent transition metal complexes, for example, Cu(I),[1] Ni(I),[2] Pd(I),[3] Cr(II),[4] Co(II),[5] and Ru(II);[6] that is, the redox potentials of the $M^{n+1}L_m/M^nL_m$ couples are shifted anodically for L = tertiary amine. Second, the stability constants of the complexes with the tertiary amines are smaller than those with primary and secondary amines.[7] Third, the d−d absorption bands of the complexes with tertiary amine ligands are shifted to the red in comparison to the analogous complexes with secondary and primary amines.[7] Finally, the central transition metal cations in complexes with tertiary amine ligands are stronger and harder acids than those in the corresponding complexes with secondary and primary amine ligands.[7]

These observations seem to indicate that tertiary amines are poorer σ-donors than their secondary and primary counterparts, a surprising conclusion as alkyls are electron-donating substituents. The more highly substituted amines should therefore be stronger σ-donors. Several plausible causes have been proposed in the literature to explain these observations:[2a,3]

* Authors to whom correspondence should be addressed. E-mail: vaneldik@chemie.uni-erlangen.de (R.v.E.); clark@chemie.uni-erlangen.de (T.C.); danmeyer@bgumail.bgu.ac.il (D.M.).

† Computer-Chemie-Centrum der Universität Erlangen-Nürnberg.

‡ Institut für Anorganische Chemie der Universität Erlangen-Nürnberg.

§ The College of Judea and Samaria.

|| Ben-Gurion University of the Negev.

(1) (a) Golub, G.; Cohen, H.; Paoletti, P.; Bencini, A.; Messori, L.; Bertini, I.; Meyerstein, D. *J. Am. Chem. Soc.* **1995**, *117*, 8353. (b) Navon, N.; Cohen, X.; Paoletti, P.; Valtancoli, B.; Bencini, A.; Meyerstein, D. *Ind. Eng. Chem. Res.* **2000**, *39*, 3536. (c) Jubran, N.; Cohen, H.; Koresh, Y.; Meyerstein, D. *J. Chem. Soc., Chem. Commun.* **1984**, 1683.

(2) (a)Wagner, F.; Barefield, E. K. *Inorg. Chem.* **1976**, *15*, 408. (b) Jubran, N.; Ginzburg, G.; Cohen, H.; Koresh, Y.; Meyerstein, D. *Inorg. Chem.* **1985**, *24*, 251. (c) Zilbermann, I.; Winnik, M.; Sagiv, D.; Rotman, A.; Cohen, H.; Meyerstein, D. *Inorg. Chim. Acta* **1995**, *240*, 503. (d) Meyerstein, D. In *Current Topics in Macrocyclic Chemistry in Japan*; Kimura, E., Ed.; Hiroshima University School of Medicine: Hiroshima, Japan, 1987; p 70.

(3) Reid, G.; Schroder, M. *Chem. Soc. Rev.* **1990**, *19*, 239.

(4) Guldi, D.; Wasgestian. F.; Meyerstein, D. *Inorg. Chim. Acta* **1992**, *194*, 15.

(5) Bertini, I.; Messori, L.; Golub, G.; Cohen, H.; Meyerstein, D. *Inorg. Chim. Acta* **1995**, *235*, 5.

(6) Che, C. M.; Wong, K. J.; Poon, C. K. *Inorg. Chem.* **1986**, *25*, 1809.

(7) (a) Meyerstein, D. *Supramol. Chem.* **1996**, *6*, 275. (b) Meyerstein, D. *Coord. Chem. Rev.* **1999**, *185−186*, 141 and references therein.

10.1021/ic0113193 CCC: $22.00
Published on Web 05/07/2002

1. The M−N bonds are elongated by steric hindrance in the complexes with tertiary amine ligands.

2. Steric hindrance affects the M−N−C bond angles and thus decreases the M−N bond strength.

3. The strain energy in the skeleton of the ligands in complexes with tertiary amine chelating ligands is expected to be larger than in those with secondary and primary amine ligands.

4. The tertiary amine ligands might induce, via steric hindrance, steric distortions (e.g. tetrahedral distortions) that could explain the stabilization of the low valent complexes for some transition metals.

However, the effect of *N*-alkylation on the solvation behavior of such complexes provides an additional explanation to these structural arguments. The tertiary amine ligands are expected to decrease the solvation energy of the complexes, thus stabilizing the low valent complexes. The effect of *N*-alkylation on the solvation energies could have two possible sources:[7]

1. *N*-Alkylation increases the radii of the complexes, thus decreasing the solvation energies.

2. Complexes with tertiary amine ligands do not have M−N−H$\cdots$$OH_2$ hydrogen bonds. The absence of these hydrogen bonds decreases the outer sphere solvation energy, decreases the electron density on the nitrogens, thus decreasing their σ-donating properties, and decreases the charge delocalization, thus transforming the central cation into a stronger and harder acid.

The structural arguments suggest that the difference between complexes with tertiary amine ligands and the analogous complexes with secondary or primary amine ligands is an inherent property of the complex and should also be observed in the gas phase. On the other hand, the solvation argument suggests that the experimental observations are specific for aqueous solutions, or for ion pairs in solvents with low dielectric constants, and that in the gas phase the tertiary amine ligands are stronger σ-donors, with all the expected consequences, than secondary or primary amine ligands. Indeed, experimental results in one system,[8] and semiempirical calculations in another,[1a] indicate that tertiary amine ligands are better σ-donors in the gas phase. These results thus suggest that solvation largely accounts for the difference in the properties of complexes with secondary and tertiary amine ligands.

We have therefore used density functional theory (DFT) to investigate the gas and solution phase behaviors of some representative complexes in order to resolve the question whether tertiary amines are inherently poor σ-donors or the observed effects are caused by solvation phenomena. Calculations present a unique opportunity to investigate the redox behavior, geometries, and electronic and electrostatic properties of the complexes and, thus, to identify the main reasons for the unusual effects of *N*-alkylation of the amine ligands.

For this purpose, the complexes of Ni(I), Ni(II), Cr(II), and Cr(III) with 1,4,8,11-tetraazacyclotetradecane (L^1 = cyclam) and with 1,4,8,11-tetramethyl-1,4,8,11-tetraaza-cyclo-tetradecane (L^2 = tetramethylcyclam, see Scheme 1) in the gas phase and in aqueous solutions were studied. These complexes were chosen because their redox potentials are known.[2,4] The results indeed strongly suggest that solvation largely accounts for the difference between the properties of the complexes as a result of *N*-alkylation of these ligands.

Scheme 1

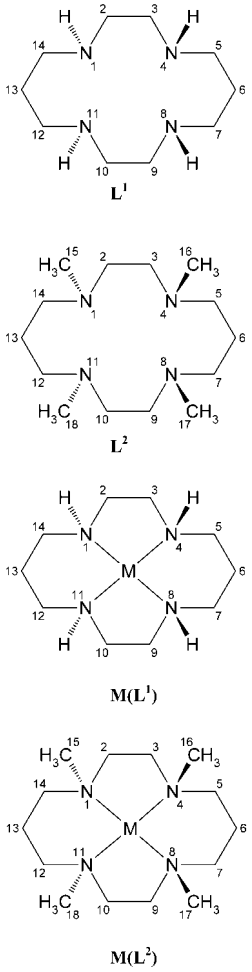

Computational Methods

All calculations were performed using Gaussian 98[9] with the B3LYP[10,11] three parameter hybrid density functional. Open shell

(8) Deng, H.; Kebarbe, P. *J. Am. Chem. Soc.* **1998**, *120*, 2925.

(9) Frisch, M. J.; Trucks, G. W.; Schlegel, H. B.; Scuseria, G. E.; Robb, M. A.; Cheeseman, J. R.; Zakrzewski, V. G.; Montgomery, J. A., Jr.; Stratmann, R. E.; Burant, J. C.; Dapprich, S.; Millam, J. M.; Daniels, A. D.; Kudin, K. N.; Strain, M. C.; Farkas, O.; Tomasi, J.; Barone, V.; Cossi, M.; Cammi, R.; Mennucci, B.; Pomelli, C.; Adamo, C.; Clifford, S.; Ochterski, J.; Petersson, G. A.; Ayala, P. Y.; Cui, Q.; Morokuma, K.; Malick, D. K.; Rabuck, A. D.; Raghavachari, K.; Foresman, J. B.; Cioslowski, J.; Ortiz, J. V.; Stefanov, B. B.; Liu, G.; Liashenko, A.; Piskorz, P.; Komaromi, I.; Gomperts, R.; Martin, R. L.; Fox, D. J.; Keith, T.; Al-Laham, M. A.; Peng, C. Y.; Nanayakkara, A.; Gonzalez, C.; Challacombe, M.; Gill, P. M. W.; Johnson, B. G.; Chen, W.; Wong, M. W.; Andres, J. L.; Head-Gordon, M.; Replogle, E. S.; Pople, J. A. *Gaussian 98*, revision A.5; Gaussian, Inc.: Pittsburgh, PA, 1998.

(10) (a) Becke, A. D. *J. Chem. Phys.* **1993**, *98*, 1372−1377, 5648−5652. (b) Stevens, P. J.; Devlin, F. J.; Chabalowski, C. F.; Frisch, M. J. *J. Phys. Chem.* **1994**, *98*, 11623−11627.

(11) Lee, C.; Yang, W.; Parr, R. G. *Phys. Rev.* **1988**, *B37*, 785−789.

Table 1. Calculated and Experimental Metal−Nitrogen and Metal−Oxygen Bond Lengths[a] (Å)

		M−N		M−O	
complex	point group	calcd	exptl	calcd	exptl
$Ni^{I}(L^{1})$	C_{2h}	2.100			
$Ni^{I}(L^{2})$	C_{2h}	2.163	2.120, 2.095		
$Ni^{II}(L^{1})$	C_{2h}	1.982	1.950, 1.929		
$Ni^{II}(L^{2})$	C_{2}	2.046, 2.041	1.991, 1.989		
$Cr^{II}(L^{1})$	C_{2h}	2.112			
$Cr^{II}(L^{2})$	C_{2h}	2.159			
$Cr^{III}(L^{1})$	C_{2h}	2.085	2.061, 2.059 2.067, 2.059		
$Cr^{III}(L^{2})$	C_{2}	2.075, 2.145			
$Ni^{I}(L^{1})\cdot 2H_2O$	C_i	2.083, 2.108		(4.108)	
$Ni^{I}(L^{2})\cdot 2H_2O$	C_{2h}	2.161		3.612	
$Ni^{II}(L^{1})\cdot 2H_2O$	C_1	1.962, 1.965, 1.972, 1.974		(3.537, 3.903)	
$Ni^{II}(L^{2})\cdot 2H_2O$	C_2	2.038, 2.036		3.540	
$Cr^{II}(L^{1})\cdot 2H_2O$	C_2	2.124, 2.123		2.624	
$Cr^{II}(L^{2})\cdot 2H_2O$	C_s	2.186, 2.169		2.529, 3.467	
$Cr^{III}(L^{1})\cdot 2H_2O$	C_2	2.100, 2.089		2.075	
$Cr^{III}(L^{1})Cl_2$			2.061, 2.059		
$Cr^{III}(L^{1})H_2O/OH$			2.067, 2.059		1.977, 1.988
$Cr^{III}(L^{2})\cdot 2H_2O$	C_2	2.176, 2.175		2.057	
$Ni^{I}(L^{1})\cdot 6H_2O$	C_1	2.100, 2.084, 2.099, 2.078		(3.741, 3.712)	
$Ni^{II}(L^{1})\cdot 6H_2O$	C_1	1.977, 1.973, 1.972, 1.964		(3.461, 3.336)	
$Cr^{II}(L^{1})\cdot 6H_2O$	C_1	2.139, 2.131, 2.103, 2.116		2.286, (3.377)	
$Cr^{III}(L^{1})\cdot 6H_2O$	C_1	2.105, 2.097, 2.096, 2.093		2.017, 2.016	

[a] Values in parentheses are the shortest distances as in these cases a bond cannot be assigned unequivocally.

species used the unrestricted formalism. All nickel complexes were calculated in their low-spin states, and all chromium complexes, as high spin. Geometries were optimized without constraints using the Schäfer−Horn−Ahlrichs split-valence basis set,[12] augmented with a set of d-type polarization functions with exponents of 0.600 and 0.864 on C and N, respectively, and p- and f-type functions with exponents of 0.086 and 0.870 on Cr and 0.111 and 1.290 on Ni.[13] This basis set combination has been found to perform particularly well for the type of problem considered here.[14] Polarized continuum model [15] calculations were used to simulate a bulk water environment at a temperature of 298.15 K. Because of the size of the systems considered, the calculations used a fixed van der Waals' surface with UFF-atomic radii[16] and 60 initial tesserae per sphere in pentakisdodecahedral patterns. Tests with the smaller complexes gave results less than 0.1 kcal mol^{-1} (total energy) different from those obtained with the self-consistent isodensity surface technique,[17] so that we conclude that the more economical method is reliable for this problem. All calculations used an initial geometry corresponding to the all *trans* conformation found to be most stable by Bultinck et al.[18] No other conformations were considered.

Results and Discussion

To resolve the questions raised in the Introduction, the optimal structures of the complexes and ligands were calculated. For most of the complexes, the stuctures in the presence of some (2−6) water molecules were also optimized. The results are presented and discussed in the following sequence: optimized geometries of the anhydrous complexes; the effect of water on these geometries; ionization potentials; reorganization energies; steric effects of the *N*-methyl substituents; and molecular electrostatic potential surfaces.

Geometries of the Anhydrous Complexes. The more important structural parameters of the optimized geometries are summarized in Table 1, and the geometries for the Ni(I) complexes are shown in Figure 1. The $Ni^{I}(L^{1})$ and $Ni^{I}(L^{2})$ complexes show square planar coordination with Ni−N bond lengths of 2.100 and 2.163 Å, respectively. The N−Ni−N angles within the rings defined by the three-carbon bridges are 94.6° and 94.0°, and those within the smaller rings are 85.4° and 86.0°, respectively, giving perfect planar coordination geometries at Ni(I). The C−N−C angles are 114.1° and 110.3°, respectively. The N−N distances are 3.088 and 3.163 Å for the long, and 2.848 and 2.952 Å for the short bridges, respectively. For comparison, the crystal structure data of $Ni^{I}(L^{2})$[19] are also included in the table. The results clearly demonstrate that, although the calculations are for the gas phase, the results resemble the measured crystal structure. The shorter M−N bonds and N−N distances in the crystal

(12) Schaefer, A.; Horn, H.; Ahlrichs, R. *J. Chem. Phys.* **1992**, *97*, 2571−2577.
(13) (a) Huzinaga, S. *Gaussian Basis Sets for Molecular Calculations*; Elsevier: Amsterdam, 1984. (b) Raghavachari, K.; Trucks, G. W. *J. Chem. Phys.* **1989**, *91*, 1062−1065.
(14) Hartmann, M.; Clark, T.; van Eldik, R. *J. Am. Chem. Soc.* **1997**, *119*, 7843.
(15) Miertus, S.; Scrocco, E.; Tomasi, J. *Chem. Phys.* **1981**, *55*, 117.
(16) (a) Rappé, A. K.; Casewit, C. J.; Colwell, K. S.; Goddard, W. A., III; Skiff, W. M. *J. Am. Chem. Soc.* **1992**, *114*, 10024. (b) Rappé, A. K.; Goddard, W. A., III. *J. Phys. Chem.* **1991**, *95*, 3358.
(17) Foresman, J. B.; Keith, T. A.; Wiberg, K. B.; Snoonian, J.; Frisch, M. J. *J. Phys. Chem.* **1996**, *100*, 16089.
(18) Bultinck, P.; Van Alsenoy, C.; Goeminne, A.; Van de Vondel, D. *J. Phys. Chem. A* **2000**, *104*, 11801−11809.
(19) Ram, M. S.; Riordan, C. G.; Ostrander, R.; Rheingold, A. L. *Inorg. Chem.* **1995**, *34*, 5884

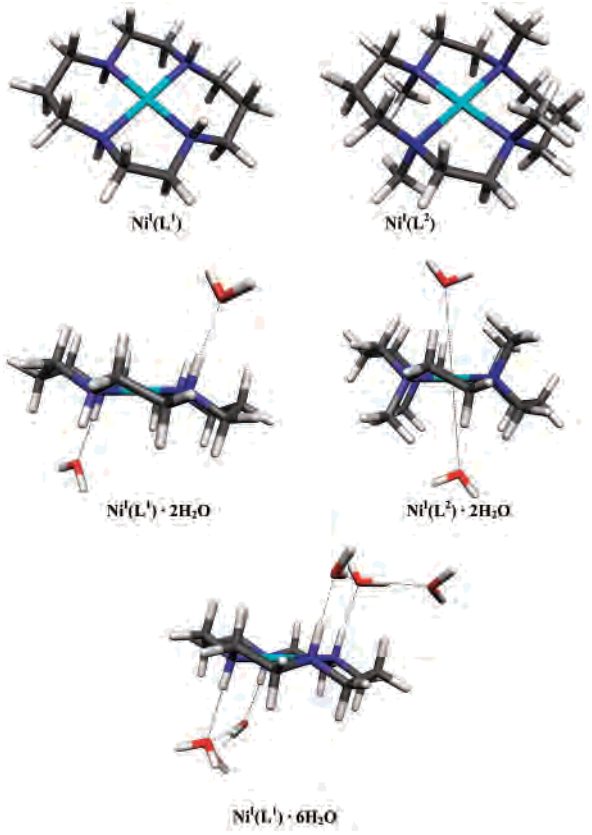

Figure 1. Calculated structures of the nickel(I) complexes.[23]

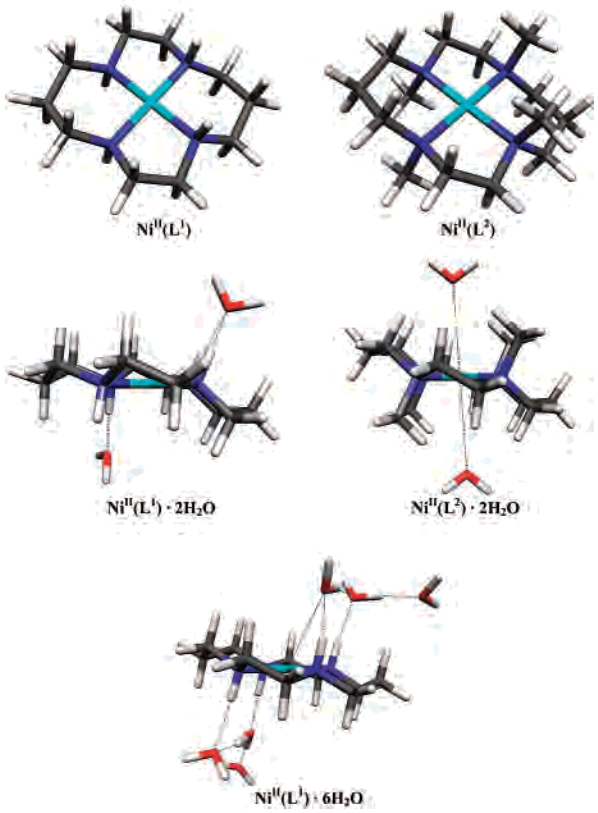

Figure 2. Calculated structures of the nickel(II) complexes.[23]

structure are expected because of the electrostatic fields in the crystal and are in the same direction as those observed for the effect of hydration water molecules for Ni^{II}(L^1), vide infra.

One-electron oxidation of Ni^{I}(L^1) and Ni^{I}(L^2) results in the shortening of the Ni−N bond lengths to a constant 1.982 Å for L^1, and to 2.041 and 2.046 Å for L^2 (the origin of the distortion in Ni^{II}(L^2), which is larger than that we would expect to result from imperfect geometry optimization, is unclear). The larger N−Ni−N angles decrease to 93.5° (L^1) and 93.2° (L^2), and the smaller ones increase correspondingly to 86.5° (L^1) and 86.8° (L^2), once again giving perfect planar coordination at Ni(II) (see Figure 2). The C−N−C angles are significantly decreased to 111.1° (L^1), and 107.9° and 108.0° (L^2), giving N−N distances of 2.887 and 2.717 Å (L^1), and 2.969, 2.806, and 2.812 Å (L^2), considerably shorter than those in the Ni(I) complexes. Again for comparison, the information from the crystal structures of Ni^{II}(L^1)[20] and Ni^{II}(L^2)[21] is also included in the table. Once again, the gas-phase results resemble the measured crystal structure. The shorter M−N bonds and N−N distances in the crystal structure are expected due to the electrostatic fields in the crystal and for Ni^{II}(L^1) are similar to the calculated values for Ni^{II}(L^1)(H$_2$O)$_2$, vide infra.

The Cr^{II}(L^1) and Cr^{II}(L^2) complexes have Cr−N distances of 2.112 and 2.159 Å, respectively. The N−Cr−N angles are 95.1° and 84.9° (L^1), and 94.5° and 85.5° (L^2), similar to those found for the Ni(I) complexes, and also result in perfect planar coordination at the metal (see Figure 3). The C−N−C angles are 114.2° and 110.2°, respectively, close to the corresponding values in the Ni(I) complexes. The long and short N−N distances are 3.118 and 2.850 Å (L^1), and 3.170 and 2.932 Å (L^2).

The Cr^{III}(L^1) complex has Cr−N distances of 2.085 Å and N−Cr−N angles of 96.0° and 84.0°. The C−N−C angles are changed little (at 113.3°) by one-electron oxidation of Cr^{II}(L^1), compared with the 3.8° decrease found on oxidizing the corresponding Ni(I) complex. The N−N distances are 3.099 and 2.790 Å, also very close to the corresponding values in the Cr(II) complex. For comparison, the crystal structure of Cr^{III}(L^1)(H$_2$O)(OH)$^{+}$ [22] is included in the table. The fit is again reasonable, and the experimental results can also be compared with the calculated ones for Cr^{III}(L^1)-(H$_2$O)$_6^{3+}$, vide infra.

The Cr^{III}(L^2) complex shows a significant distortion from ideal symmetrical coordination (see Figure 4). Two of the four methyl groups have a nearly eclipsed conformation to the Cr−N bonds, forming a Cr−N−C−H dihedral angle of 5.6°. The corresponding Cr−H distances are 2.112 Å, while the Cr−H distances to the other methyl groups are 3.264 and 3.397 Å. The Cr−N−C angles are 89.1° and 116.8°, compared to 114.7° in the Cr(II) complex. The N−CH$_3$ distances are 1.473 and 1.505 Å. The Cr−N bond lengths

(20) Prasad, L.; Nyburg, S. C.; McAuley, A. *Acta Crystallogr., Sect. C* **1987**, *43*, 1038.
(21) Barefield, E. K.; Freeman, G. M.; Van Derveer, D. G. *Inorg. Chem.* **1986**, *25*, 552.
(22) Palmer, R. A.; Potter, B. S.; Tarriverd, S.; Lisgarten, J. L.; Flint, C. D.; Gazi, D. M. *Acta Crystallogr., Sect. C* **1996**, *52*, 1177.

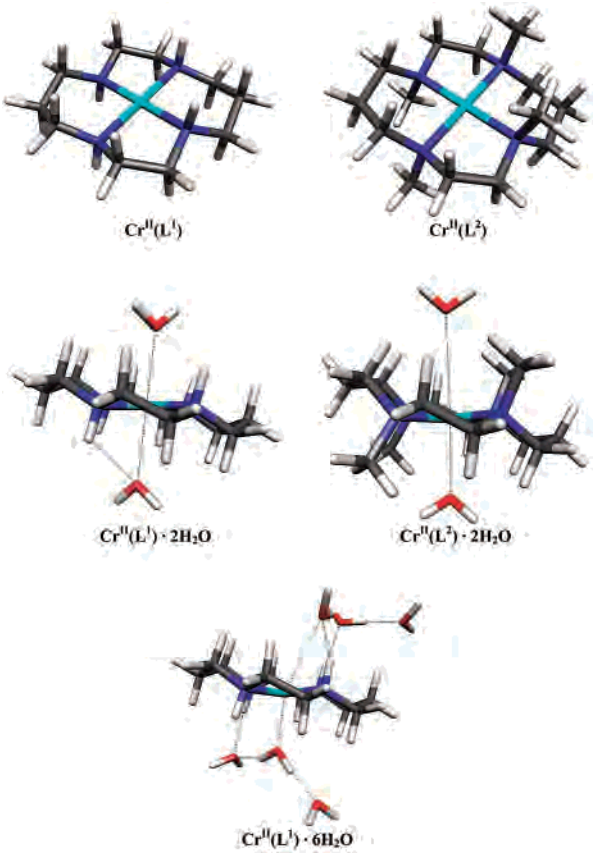

Figure 3. Calculated structures of the chromium(II) complexes.[23]

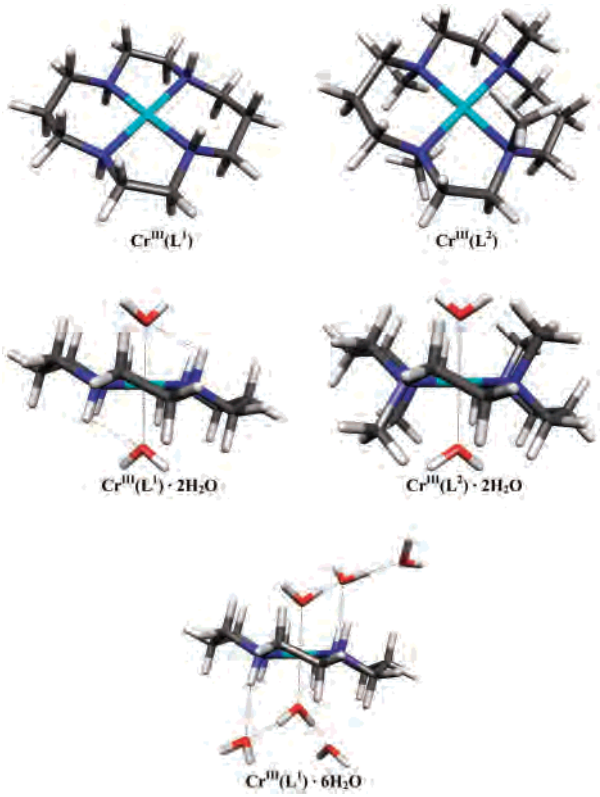

Figure 4. Calculated structures of the chromium(III) complexes.[23]

are 2.075 and 2.145 Å. The large N−Cr−N angles are 95.1°, but the smaller ones show some variation at 83.9° and 85.9°. The N−C−N angles show a corresponding small variation

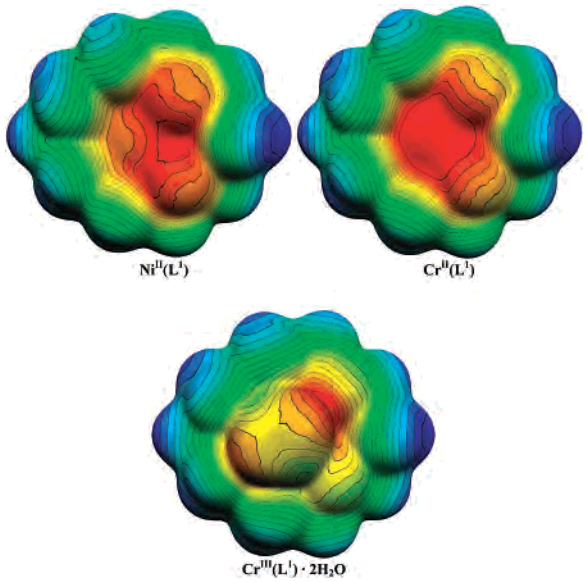

Figure 5. Isodensity surfaces (plotted at an electron density of 0.001 au) of $Ni^{II}(L^1)$, $Cr^{II}(L^1)$, and $Cr^{III}(L^1)\cdot 2H_2O$, color-coded according to the molecular electrostatic potential. The color scales range from 130 kcal·mol^{-1} (blue) to 200 kcal·mol^{-1} (red) for the $Ni^{II}(L^1)$ and $Cr^{II}(L^1)$ complexes and from 190 to 300 kcal·mol^{-1} for the $Cr^{III}(L^1)\cdot 2H_2O$ complex.[23]

with two 111.2° and two 111.0° angles. The N−N distances are 3.113, 2.773, and 2.924 Å.

The geometric properties, in particular the small Cr−H distance of 2.112 Å, indicate strong agostic interactions within the $Cr^{III}(L^2)$ complex. These interactions are especially evident from the vibrational frequencies associated with the relevant CH_3-groups. The CH-stretch vibrations associated with the agostic hydrogens are calculated to be 450−540 cm^{-1} lower in frequency than the others associated with the relevant methyl groups. Such agostic interactions are not expected to be observed experimentally because it will be extremely difficult to synthesize a planar Cr(III) complex of L^2 with no axial ligands.

Molecular Electrostatic Potential Surfaces. Figure 5 shows the isodensity surfaces (plotted at an electron density of 0.001 au) of $Ni^{II}(L^1)$, $Cr^{II}(L^1)$, and $Cr^{III}(L^1)\cdot 2H_2O$, color-coded according to the molecular electrostatic potential at the surface.[23] The color scales range from 130 to 200 kcal mol^{-1} for the $Ni^{II}(L^1)$ and $Cr^{II}(L^1)$ complexes and from 190 to 300 kcal mol^{-1} for the $Cr^{III}(L^1)\cdot 2H_2O$ complex. The color scales are different because of the different charges on the complexes, but nonetheless, Figure 5 makes very clear that the major areas of positive electrostatic potential on the surface of the Ni(II) complex can be assigned to the hydrogen bond donor hydrogens on the amine nitrogens, rather than to the metal center. In $Cr^{II}(L^1)$, on the other hand, the most positive areas of the surface are associated with the metal ion. This leads us to expect very different coordination behavior with water molecules. We therefore calculated the eight complexes treated previously with two coordinated water molecules, to simulate the specific solvation of

(23) Visualization was performed with: Flükiger, P.; Lüthi, H. P.; Portmann, S.; Weber, J. *MOLEKEL 4.0*; Swiss Center for Scientific Computing: Manno, Switzerland, 2000.

relatively strongly conserved waters, an effect that is not reproduced fully by the PCM-calculations.

Geometries of Partially Hydrated Complexes. Introduction of several solvent (water) molecules into the structures of the anhydrous systems results in dramatically different effects on the first coordination sphere in the gas phase. For the Ni complexes of L^1, the subsequent introduction of two, four, and six water molecules were calculated and show no direct binding to the metal center, as expected for low spin d^8 and monovalent Jahn−Teller distorted d^9 complexes. The water molecules form hydrogen bonds with the N−H groups (see Figures 1 and 2). When less than four water molecules are present, they tend to bridge two N−H groups, whereas, as expected, no bridging occurs for four water molecules. In the case of six water molecules, the additional two molecules hydrogen bond to the already bound water molecules. For the Ni complexes of L^2, the two water molecules are very weakly bound, as expected. The Ni−O distances are 3.612 and 3.540 Å for the Ni(I) and Ni(II) complexes, respectively. In all these Ni systems, the hydrogen bonding of the water molecules results in a shortening of the Ni−N bonds, as predicted [7] (see Table 1).

In the case of the Cr complexes of L^1, the first two water molecules become axial ligands as expected (see Figures 3 and 4). They still interact strongly with the NH groups, however. Additional water molecules hydrogen bond to the axial water ligands as these are significantly more acidic than the N−H groups and form some hydrogen bonds to the N−H groups. The axial binding of the water molecules causes a slight elongation of the Cr−N bonds as expected. In the Cr(II) complex, the Jahn−Teller effect is clearly evident from the long Cr−O bonds. It is of interest to note that in the Cr(III) complex with six water molecules, one of the axial bound water molecules is acidic enough to cause a partial proton transfer (see Figure 4). The corresponding O−H···O bond lengths are 1.072 Å for the O−H bond and 1.419 Å for the hydrogen bond. The other O−H bond of the axially bound water molecule is shortened slightly (0.973 Å). In the case of the Cr complexes of L^2, two water molecules bind axially to the metal center and result in an asymmetric Jahn−Teller distortion for Cr(II), with one relatively short and one very long Cr−O bond. The water binding results in a very slight elongation of the Cr−N bonds in analogy to the Cr(II) complex of L^1. In the Cr(III) complex of L^2, the introduction of two water molecules induces a lengthening of the Cr−N bonds and, as a result, a shortening of the Cr−O bonds in comparison to the nonmethylated complex. This makes the water molecules in Cr(III) more acidic; that is, the central cation is a harder acid.

Ionization Potentials. Table 2 shows the calculated total energies, ionization potentials, and solvation energies for the anhydrous complexes of L^1 and L^2 with the four different metal centers. The calculated gas phase adiabatic ionization potentials for the unsubstituted and tetramethyl Ni(I) complexes (8.52 and 8.66 eV, respectively) seem to indicate that there is very little substituent effect due to the four methyl groups in this case and that, if anything, the tetramethyl complex is marginally more difficult to oxidize than its unsubstituted counterpart. This is surprising, as the Ni−N bond distances are ∼0.06 Å longer in the methylated complexes, probably because of steric hindrance, which should make it considerably more difficult to oxidize. However, electron donation by the methyl substituents makes the nitrogens better σ-donors, an effect which compensates the effect of the bond elongation. For the Cr(II) complexes, however, a significant stabilization of the higher oxidation state in the tetramethyl complex is observed, leading to a lowering of the ionization potential from 16.19 to 15.38 eV. In this case, *N*-methylation on the average also elongates the Cr−N bonds, except for a slight shortening of two Cr−N bonds due to the agostic interaction with a hydrogen atom on a methyl substituent, which should make the oxidation

Table 2. Calculated Total Energies (au), Ionization Potentials (eV), and Solvation Energies (kcal mol^{-1})

metal ion	species	energy	species	energy
		Gas Phase		
Ni^I	$Ni^I(L^1)$	−2122.05946	$Ni^I(L^2)$	−2279.13719
Ni^{II}	$Ni^{II}(L^1)$	−2121.74645	$Ni^{II}(L^2)$	−2278.81910
ionization potential		8.52		8.66
Cr^{II}	$Cr^{II}(L^1)$	−1657.94805	$Cr^{II}(L^2)$	−1815.02922
Cr^{III}	$Cr^{III}(L^1)$	−1657.35314	$Cr^{III}(L^2)$	−1814.46419
ionization potential		16.19		15.38
		Polarized Continuum Model (Water)		
Ni^I	$Ni^I(L^1)$	−2122.13332	$Ni^I(L^2)$	−2279.20128
solvation energy		−46.3		−40.2
Ni^{II}	$Ni^{II}(L^1)$	−2122.01284	$Ni^{II}(L^2)$	−2279.06274
solvation energy		−167.2		−152.9
ionization potential		3.28		3.77
Cr^{II}	$Cr^{II}(L^1)$	−1658.21480	$Cr^{II}(L^2)$	−1815.27380
solvation energy		−167.4		−153.5
Cr^{III}	$Cr^{III}(L^1)$	−1657.96575	$Cr^{III}(L^2)$	−1815.00369
solvation energy		−384.4		−338.5
ionization potential		6.78		7.35
		Supermolecule Calculations with Two Water Molecules in the Gas Phase		
Ni^I	$Ni^I(L^1)\cdot 2H_2O$	−2274.77753	$Ni^I(L^2)\cdot 2H_2O$	−2431.84522
Ni^{II}	$Ni^{II}(L^1)\cdot 2H_2O$	−2274.49416	$Ni^{II}(L^2)\cdot 2H_2O$	−2431.55127
ionization potential		7.71		8.00
Cr^{II}	$Cr^{II}(L^1)\cdot 2H_2O$	−1810.69622	$Cr^{II}(L^2)\cdot 2H_2O$	−1967.76834
Cr^{III}	$Cr^{III}(L^1)\cdot 2H_2O$	−1810.21123	$Cr^{III}(L^2)\cdot 2H_2O$	−1967.28881
ionization potential		13.20		13.05
		Supermolecule Calculations with Six Water Molecules in the Gas Phase		
Ni^I	$Ni^I(L^1)\cdot 6H_2O$	−2580.22993		
Ni^{II}	$Ni^{II}(L^1)\cdot 6H_2O$	−2579.98613		
ionization potential		6.63		
Cr^{II}	$Cr^{II}(L^1)\cdot 6H_2O$	−2116.19934		
Cr^{III}	$Cr^{III}(L^1)\cdot 6H_2O$	−2115.79695		
ionization potential		10.95		

more difficult. However, the effect of the methyls on the σ-donation properties of the nitrogens is expected to increase with the oxidation state; that is, it should be considerably larger for the Cr(II) → Cr(III) than for the Ni(I) → Ni(II) oxidation, as observed. Thus, the inductive effect of the four methyl groups makes the tetramethyl Cr(II) complex 0.81 eV easier to oxidize in the gas phase than its unsubstituted equivalent.

The inclusion of two axial water molecules on the Cr complexes results in a large decrease in the ionization potentials; the effect is somewhat larger for $Cr(L^1)$ than for $Cr(L^2)$ complexes (see Table 2). This observation is in agreement with that expected when two more σ-donor ligands are bound to the metal center. Addition of further water molecules, which are only hydrogen bonded to the N−H groups in the Ni case and to the water molecules in the Cr case, to the $Ni(L^1)$ and $Cr(L^1)$ complexes results in a considerable further decrease in the ionization potential. This effect is clearly due to the charge delocalization enabled by these hydrogen bonds and to the transformation of the donor atoms in the inner coordination sphere into better σ-donors.

The calculations were repeated for a polarized continuum in order to evaluate the effect of outer sphere solvation, neglecting any specific hydrogen bonding interactions. The results for the anhydrous complexes reveal that the outer sphere solvation has a major effect on the ionization potentials. The ionization potential for $Ni^I(L^1)$ is decreased by 5.24 eV, whereas for $Ni^I(L^2)$ the potential is decreased by 4.89 eV. This difference is clearly due to the larger radii of the *N*-methylated complexes. As a result, $Ni^I(L^2)$ is a weaker reducing agent than $Ni^I(L^1)$ by 0.49 eV, in reasonable agreement with the experimental results, viz. 0.43 eV.[2b] As expected, the outer sphere solvation energies for the higher charged Cr complexes are larger, viz. 9.41 for $Cr^{II}(L^1)$ and 8.03 eV for $Cr^{II}(L^2)$. Clearly also the effect of *N*-methylation is larger in this case, that is, making the $Cr^{II}(L^2)$ complex a weaker reducing agent in aqueous solution than $Cr^{II}(L^1)$ by 0.57 eV. The observed trend is in accord with the experimental results; however, the value is significantly smaller than the observed value of 1.1 eV.[4] This comparison is made for the $M(L)^{(n+1/n)}$ couples and not for the supermolecules. The effect of the first two waters is large and specific for the chromium complexes, so that the continuum calculations do not reproduce the whole solvent effect. However, similar calculations using continuum solvation for the hydrated systems give inconsistent results because of the deep clefts found in the molecular surface.

Reorganization Energies. The reorganization energies, that is, the difference between the vertical and adiabatic oxidation processes for the anhydrous Ni complexes, were calculated (see Table 3). The results indicate that the reorganization energies are very similar for the complexes with L^1 and L^2, which corroborates earlier suggestions that the higher self-exchange rate of $Ni(L^2)$ than $Ni(L^1)$ is attributable to the difference in the outer sphere solvation contribution.[7]

Steric Effects of the Methyl Groups. The metal-induced strain energies of the ligands, that is, the difference between the energies of the ligand in its coordinated geometry and its free optimal configuration, as shown in Figure 6, were calculated (Table 4). This was accomplished by performing a single point energy calculation for the optimized complex structures following removal of the metal center. The results clearly indicate that the metal-induced strain energies of the ligands are significantly smaller for the *N*-methylated ligand in all the complexes studied. This surprising result plausibly

Table 3. Calculated Total Energies (au), Vertical Ionization Potentials (eV), and Reorganization Energies (kcal mol^{-1})

	geometry		reorganization energy
	$Ni^I(L^1)$	$Ni^{II}(L^1)$	
Ni^I	−2122.05946	−2122.04523	8.9
Ni^{II}	−2121.73233	−2121.74645	8.9
ionization potential	8.90	8.13	$\lambda_{in} = 17.8$

	geometry		reorganization energy
	$Ni^I(L^2)$	$Ni^{II}(L^2)$	
Ni^I	−2279.13719	−2279.12247	9.2
Ni^{II}	−2278.80545	−2278.81910	8.6
ionization potential	9.03	8.26	$\lambda_{in} = 17.8$

	geometry		reorganization energy
	$Ni^I(L^1)\cdot 2H_2O$	$Ni^{II}(L^1)\cdot 2H_2O$	
Ni^I	−2274.77753	−2274.75922	11.5
Ni^{II}	−2274.47701	−2274.49416	10.8
ionization potential	8.18	7.21	$\lambda_{in} = 22.3$

	geometry		reorganization energy
	$Ni^I(L^2)\cdot 2H_2O$	$Ni^{II}(L^2)\cdot 2H_2O$	
Ni^I	−2431.84522	−2431.82877	10.3
Ni^{II}	−2431.53573	−2431.55127	9.8
ionization potential	8.42	7.55	$\lambda_{in} = 20.1$

	geometry		reorganization energy
	$Cr^{II}(L^1)$	$Cr^{III}(L^1)$	
Cr^{II}	−1657.94805	−1657.94561	1.5
Cr^{III}	−1657.35083	−1657.35314	1.5
ionization potential	16.25	16.12	$\lambda_{in} = 3.0$

	geometry		reorganization energy
	$Cr^{II}(L^2)$	$Cr^{III}(L^2)$	
Cr^{II}	−1815.02922	−1814.99526	21.3
Cr^{III}	−1814.45399	−1814.46419	6.4
ionization potential	15.65	14.45	$\lambda_{in} = 27.7$

	geometry		reorganization energy
	$Cr^{II}(L^1)\cdot 2H_2O$	$Cr^{III}(L^1)\cdot 2H_2O$	
Cr^{II}	−1810.69622	−1810.65987	22.8
Cr^{III}	−1810.17417	−1810.21123	23.3
ionization potential	14.21	12.21	$\lambda_{in} = 46.1$

	geometry		reorganization energy
	$Cr^{II}(L^2)\cdot 2H_2O$	$Cr^{III}(L^2)\cdot 2H_2O$	
Cr^{II}	−1967.76834	−1967.72789	25.4
Cr^{III}	−1967.24369	−1967.28881	28.3
ionization potential	14.28	11.95	$\lambda_{in} = 53.7$

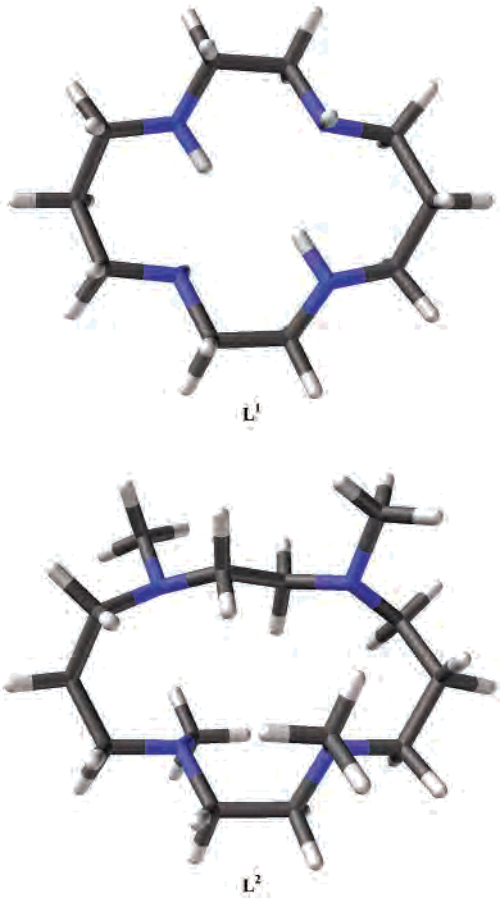

Figure 6. Minimum structures of cyclam (L^1) and tetramethylcyclam (L^2).[23]

Table 4. Calculated Total Energies (au) and Strain Energies (kcal mol^{-1}) of the Ligands Compared to the Free Ligand

ligand	geometry	total energy	strain energy
L^1	L^1	−613.99052	0.0
L^1	$Cr^{II}(L^1)$	−613.93997	31.7
L^1	$Cr^{III}(L^1)$	−613.92977	38.1
L^1	$Ni^{I}(L^1)$	−613.94944	25.8
L^1	$Ni^{II}(L^1)$	−613.93071	37.5
L^2	L^2	−771.06520	0.0
L^2	$Cr^{II}(L^2)$	−771.03296	20.2
L^2	$Cr^{III}(L^2)$	−771.01445	31.8
L^2	$Ni^{I}(L^2)$	−771.04305	13.9
L^2	$Ni^{II}(L^2)$	−771.01636	30.6

stems from the longer M−N bonds in the complexes of the *N*-methylated ligand, which seem to relieve some strain in the macrocyclic structure. It should naturally be noted that in this calculation the difference between the strain energies of the ligated and free ligands is evaluated, and it is reasonable to assume that the strain energy in free L^2 is considerably larger than in free L^1. This result points out that the lower stability constants of macrocyclic tertiary amine ligands as compared to the corresponding secondary amine ligands do not originate from strain energies and must therefore be attributed to outer sphere solvation effects.

Figures 7 and 8 show the van der Waals' surfaces of the eight complexes studied, color-coded in order to visualize the accessible surface area assignable to the metal ion.[24] The effect of the methyl groups is more pronounced for the higher oxidation state of each metal. In $Ni^{II}(L^2)$ and $Cr^{III}(L^2)$, the

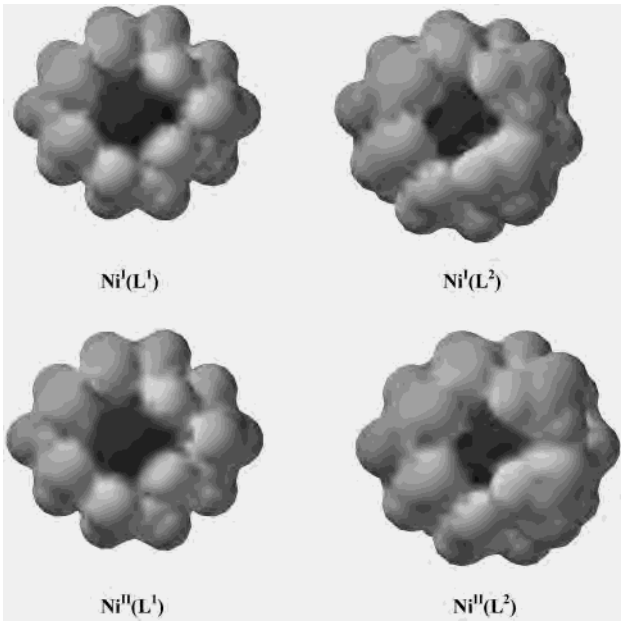

Figure 7. van der Waals' surfaces for the unsubstituted and tetramethyl nickel complexes. The dark areas are assigned to the metal ion.

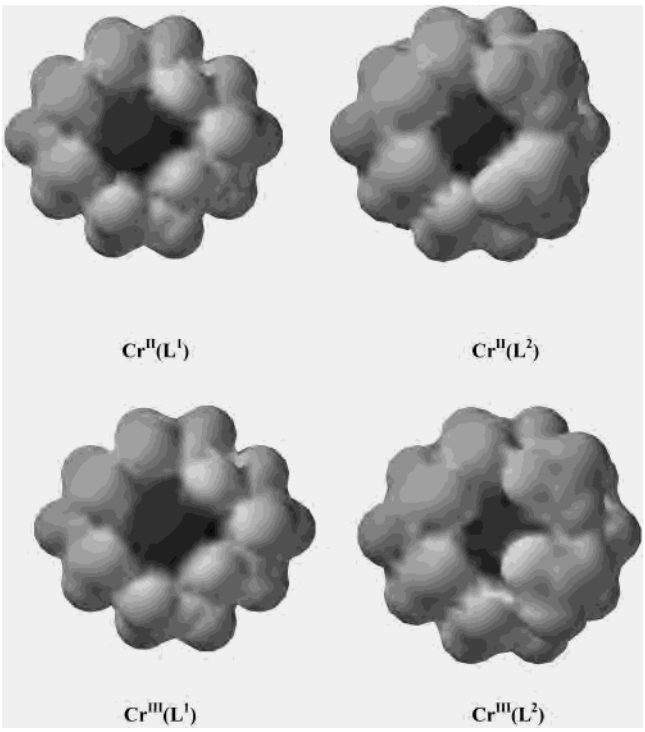

Figure 8. van der Waals' surfaces for the unsubstituted and tetramethyl chromium complexes. The dark areas are assigned to the metal ion.

accessible area assigned to the metal ion is reduced by 50% or more on tetramethyl substitution. Furthermore, the areas assigned to the metal ions lie in fairly deep pockets that are not accessible to large solvent molecules, so that the methyl groups restrict the access of the solvent to the metal ions

(24) The plots were produced by assigning an artificial point charge of +1 to the metal ion and zero charges to all other atoms and then using these charges to calculate a virtual electrostatic potential at the surface. The potential thus falls off reciprocally with the distance from the metal ion and gives a good representation of the area of the molecule assignable to the metal.

very significantly compared with the unsubstituted complexes. This effect should lead to very much less effective solvation of the *N*-methylated complexes.

Concluding Remarks

The following conclusions can be drawn from the results reported:

1. Outer sphere solvation effects mainly account for the effect of *N*-alkylation on the redox potential of transition metal complexes with secondary amine ligands.

2. Tertiary amine ligands induce steric hindrance which results in the elongation of the metal−nitrogen bonds and in a decrease in the strain energies of the ligands.

3. The calculations point out that the lower stability constants of macrocyclic tertiary amine complexes, in comparison to secondary amine complexes, originate from outer sphere solvation effects and not from ligand strain energy.

4. *N*-Alkylation causes the nitrogen donors to become better σ-donors as can be seen from the ionization potentials of the anhydrous Cr complexes in the gas phase.

5. Water hydrogen bonding to the secondary amine ligands increases the σ-donation properties of the nitrogen donors as is evident from the shortening of the Ni−N bond.

6. Axial binding of water molecules in the Cr complexes elongates the metal−nitrogen bond.

7. Outer sphere water hydrogen bonding of the type M−X−H···OH_2, X = N or O, significantly lowers the ionization potentials of the central cation because of charge delocalization and strengthening of the σ-donation properties of X.

8. The considerably longer Cr−N bonds in $Cr^{III}(L^2)(H_2O)_2^{3+}$ than in $Cr^{III}(L^1)(H_2O)_2^{3+}$ result in considerably shorter Cr−O bonds for $Cr^{III}(L^2)(H_2O)_2^{3+}$; that is, *N*-alkylation increases the hardness of the metal center.

9. In none of the complexes studied does *N*-alkylation induce a tetrahedral distortion as proposed in some studies.

The results point out that *N*-alkylation causes several contradictory effects. On one hand, the nitrogens become better σ-donors which shifts the redox potential of the couples cathodically; on the other hand, solvational effects and steric effects shift the potential anodically. Because the solvational effects are larger, *N*-alkylation generally stabilizes low valent transition metal complexes.

Acknowledgment. The authors gratefully acknowledge financial support from the Deutsche Forschungsgemeinschaft as part of Sonderforschungsbereich 583, "Redox-Active Metal Complexes: Control of Reactivity via Molecular Architecture", and a research award from the Alexander von Humboldt Foundation to D. M.

Supporting Information Available: Cartesian coordinates, total energies, and zero-point energies of all structures described in the text as archive entries produced by Gaussian 98. This material is available free of charge via the Internet at http://pubs.acs.org.

IC0113193